

Suppression of globular cluster formation in metal-poor gas clouds by Lyman-alpha radiation feedback

Makito Abe^{1*} and Hidenobu Yajima^{2,3}

¹Center for Computational Sciences, University of Tsukuba, Ten-nodai, 1-1-1 Tsukuba, Ibaraki 305-8577, Japan

²Frontier Research Institute for Interdisciplinary Sciences, Tohoku University, Sendai 980-8578, Japan

³Astronomical Institute, Tohoku University, Sendai 980-8578, Japan

Accepted ?; Received ??; in original form ???

ABSTRACT

We study the impact of Ly α radiation feedback on globular cluster (GC) formation. In this Letter, we analytically derive the relation between star formation efficiency (SFE) and metallicity in spherical clouds with the Ly α radiation feedback. Our models show that the SFE becomes small as the metallicity decreases. In metal-poor gas clouds, Ly α photons are trapped for a long time and exert strong radiation force to the gas, resulting in the suppression of star formation. We find that bound star-clusters (SFE $\gtrsim 0.5$) form only for the metallicity higher than $\sim 10^{-2.5} Z_{\odot}$ in the case with the initial cloud mass $10^5 M_{\odot}$ and the radius 5 pc. Our models successfully reproduce the lower bound of observed metallicity of GCs. Thus, we suggest that the Ly α radiation feedback can be essential in understanding the formation of GCs.

Key words: globular clusters: general – radiative transfer – dust, extinction – galaxies: formation – galaxies: high-redshift

1 INTRODUCTION

Star formation in the early Universe is poorly known due to little direct observations. Globular clusters (GCs) are key objects to understand the early Universe, because most of them were likely formed more than ~ 10 billion years ago (e.g., Krauss & Chaboyer 2003; Dotter et al. 2007; Vandenberg et al. 2013). However, the formation mechanism of GCs has not been understood yet. Very recently, Vanzella et al. (2017) observed a young and compact object at $z \sim 6$ of which the physical properties were similar to that of GCs (see also Bouwens et al. 2017). In addition, Renzini (2017) discussed the detectability of GC progenitors in the early Universe by *James Webb Space Telescope (JWST)*. Therefore, the theoretical study of physical conditions for the GC formation is timely just before the JWST era. An interesting feature of observed GCs is that the typical metallicity is lower than the solar neighbourhood, but limited at $\log Z/Z_{\odot} \gtrsim -2.5$ (Puzia et al. 2005). On the other hand, single metal-poor stars show a wide metallicity range extended to $\log Z/Z_{\odot} < -4$ (Aoki et al. 2007; Yong et al. 2013). In this work, we study the origin of the lower bound of the observed metallicity of GCs and key physics regulating their formations.

Theoretically, cosmological N -body simulations successfully reproduced the distribution of GCs in our Milky

Way with sub-grid models (Diemand et al. 2005; Moore et al. 2006; Trenti et al. 2010). High-resolution cosmological hydrodynamics simulations showed that merging process of high-redshift dwarf galaxies induced the formation of compact clouds where were likely to be formation sites of GCs (e.g., Kravtsov & Gnedin 2005; Ricotti et al. 2016; Kim et al. 2017). Abe et al. (2016) suggested that compact gas clouds were also formed under the strong ultraviolet (UV) background radiation by using the radiative-hydrodynamics simulations (see also, Hasegawa et al. 2009). Thus, recent hydrodynamics simulations have been able to resolve the formation of compact gas clouds. On the other hand, the formation mechanism of GCs in the compact clouds remains unknown. Once stars form, the internal stellar feedback can disrupt the clouds, resulting in suppression of star formation (e.g., Geen et al. 2017). Therefore, the internal feedback has to be considered to understand the formation of GCs.

We here consider Ly α radiation as the internal feedback. Due to its large cross-sections and the resonant scattering nature, Ly α photons would be trapped for a long time in a star-forming cloud and exert strong radiation force to the gas (Rees & Ostriker 1977; Cox 1985; Oh & Haiman 2002; Yajima & Khochfar 2014, 2017). Such Ly α radiation feedback in the high- z star-forming galaxies has been argued by using radiative transfer simulations (Dijkstra & Loeb 2008), or one-dimensional Ly α radiative-hydrodynamics simulations (Smith et al. 2017). These works revealed that the Ly α radiation feedback induced the outflow of gas from the low-

* E-mail: mabe@ccs.tsukuba.ac.jp

mass protogalaxies with the halo masses of $M_h \lesssim 10^8 M_\odot$. This can cause the quench of star formation. Therefore, Ly α radiation feedback may also play a roll even in the formation of GCs.

On the other hand, as the gas is metal-enriched, Ly α photons are absorbed by dust in the cloud. Even in low-metal gas clouds, the dust reduces the number density of trapped Ly α photons, and make the Ly α feedback ineffective. The impacts of Ly α radiation feedback on the GC formation in low-metallicity gas clouds has not been investigated. In this work, we study the conditions for the formation of GCs by taking into account the Ly α radiation feedback with the dust absorption.

2 STAR FORMATION IN SPHERICAL GAS CLOUDS UNDER THE Ly α RADIATIVE FEEDBACK

In this work, we consider star formation in spherical gas clouds with the mass M_{cl} and the radius r_{cl} . As the star formation proceeds, massive stars form H II bubbles in a cloud. In the H II region, Ly α photons are produced via recombination processes, and can exert radiation force on the cloud. We study the regulation of star formation due to the Ly α radiation force under the assumption of a single point source at the centre of the cloud, and derive the physical conditions for the GC formation.

In the equilibrium state, Ly α luminosity is simply proportional to ionizing photon emissivity as $L_{\text{Ly}\alpha} = 0.68\epsilon_{\text{Ly}\alpha}\dot{N}_{\text{ion}}$, where $\epsilon_{\text{Ly}\alpha} = 10.2$ eV is the energy of each Ly α photon, and \dot{N}_{ion} is the ionizing photon emissivity from a star cluster (Yajima et al. 2012). When the age of star cluster is younger than the lifetime of massive stars, the ionizing photon emissivity is proportional to the stellar mass $M_* = \epsilon M_{\text{cl}}$, where ϵ denotes the star formation efficiency (SFE) of the cloud. Under the assumption of the Salpeter initial mass function (IMF) with the mass range of 0.1 – 100 M_\odot and the metallicity of $Z/Z_\odot = 0.01$, the ionizing photon emissivity per solar mass \dot{n}_{ion} is evaluated as $\sim 4.1 \times 10^{46} \text{ s}^{-1} M_\odot^{-1}$ at the age of 1 Myr (Chen et al. 2015). On the other hand, if we adopt the Larson IMF with its characteristic mass $M_{\text{ch}} = 1 M_\odot$, the ionizing photon emissivity somewhat increases, resulting in $\dot{n}_{\text{ion}} \sim 1.1 \times 10^{47} \text{ s}^{-1} M_\odot^{-1}$. Thus, we evaluate the Ly α luminosity in the cloud as

$$L_{\text{Ly}\alpha} = 1.1 \times 10^{36} \text{ erg s}^{-1} \epsilon \left(\frac{\dot{n}_{\text{ion}}}{1 \times 10^{47} \text{ s}^{-1} M_\odot^{-1}} \right) \left(\frac{M_{\text{cl}}}{M_\odot} \right). \quad (1)$$

Next, we estimate the Ly α radiation force enhanced due to multiple scattering processes as (Dijkstra & Loeb 2008)

$$F_{\text{rad}}^{\text{Ly}\alpha} \sim \frac{t_{\text{trap}}}{t_{\text{cross}}} \frac{L_{\text{Ly}\alpha}}{c} \equiv f_{\text{boost}} \frac{L_{\text{Ly}\alpha}}{c}, \quad (2)$$

where c is the speed of light, t_{trap} is the trapping time of Ly α photons in a cloud, $t_{\text{cross}} = r_{\text{cl}}/c$ is the light crossing time, and

$$f_{\text{boost}} = \frac{t_{\text{trap}}}{t_{\text{cross}}} = \frac{c}{r_{\text{cl}}} t_{\text{trap}} \quad (3)$$

is the boost factor of the radiation force due to multiple scattering processes. According to the numerical study (Adams

1975), the trapping time $t_{\text{trap,H}}$ can be expressed by the optical depth at the line center frequency τ_0 as

$$t_{\text{trap,H}} \sim \begin{cases} 15 t_{\text{cross}} & \text{for } 10^3 < \tau_0 < 10^{5.5} \\ 15 \left(\frac{\tau}{10^{5.5}} \right)^{\frac{1}{3}} t_{\text{cross}} & \text{for } \tau_0 \geq 10^{5.5}. \end{cases} \quad (4)$$

As the photon density increases, the Ly α radiation force pushes the cloud outward and prevents it to contract. When the Ly α radiation force exceeds the gravitational force, i.e., $F_{\text{Ly}\alpha} > F_{\text{grav}}$, the gas is likely to be evacuated, resulting in the quenching of star formation. This condition is described as

$$f_{\text{boost}} \frac{L_{\text{Ly}\alpha}}{c} > G \frac{(1-\epsilon)M_{\text{cl}}^2}{r_{\text{cl}}^2}. \quad (5)$$

Thus, by substituting Eq. (1) into Eq. (5), we obtain the boost factor to suppress the star formation as a function of $\xi \equiv \epsilon/(1-\epsilon)$ (corresponding to ‘‘stellar-to-gas mass ratio’’):

$$f_{\text{boost}} > 3.0 \xi^{-1} \left(\frac{\dot{n}_{\text{ion}}}{1 \times 10^{47} \text{ s}^{-1} M_\odot^{-1}} \right)^{-1} \left(\frac{M_{\text{cl}}}{10^5 M_\odot} \right) \left(\frac{r_{\text{cl}}}{5 \text{ pc}} \right)^{-2}. \quad (6)$$

In order to estimate f_{boost} , we calculate the trapping time of the Ly α photons. The optical depth from the cloud centre to the edge is estimated as

$$\tau_0 = 7.1 \times 10^9 \left(\frac{M_{\text{cl}}}{10^5 M_\odot} \right) \left(\frac{r_{\text{cl}}}{5 \text{ pc}} \right)^{-2}. \quad (7)$$

By considering the condition $\tau_0 > 10^{5.5}$ in Eq. (4), this results in

$$t_{\text{trap,H}} = 6.9 \times 10^3 \text{ yr} \left(\frac{M_{\text{cl}}}{10^5 M_\odot} \right)^{1/3} \left(\frac{r_{\text{cl}}}{5 \text{ pc}} \right)^{1/3}. \quad (8)$$

Thus, according to Eq. (3) and (8), the boost factor is given by

$$f_{\text{boost,H}} = 4.2 \times 10^2 \left(\frac{M_{\text{cl}}}{10^5 M_\odot} \right)^{1/3} \left(\frac{r_{\text{cl}}}{5 \text{ pc}} \right)^{-2/3}. \quad (9)$$

As the metallicity increases, the trapping time can be shorter than the estimation in Eq. (4) by taking into account the dust absorption of Ly α photons during the journey. The mean free path of the Ly α photons regarding the dust absorption l_d is $l_d = 1/(\sigma_d n_d)$, where

$$\sigma_d n_d = \pi a_d^2 Q_{\text{d,abs}} n_{\text{H}} \left(\frac{m_{\text{H}}}{m_{\text{d}}} \right) f_{\text{d}} \left(\frac{Z}{Z_\odot} \right). \quad (10)$$

Here, a_d represents the dust size, $Q_{\text{d,abs}}$ is the absorption efficiency to the geometrical cross section, f_{d} is the dust-to-gas mass ratio at the metallicity of solar abundance, n_{H} and m_{H} are hydrogen number density and hydrogen mass. We set $Q_{\text{d,abs}} = 1$, which is reasonable when the wavelength of photons is shorter than $\sim 2\pi a_d$ (Draine & Lee 1984). As a fiducial value, we set $f_{\text{d}} = 0.01$ that is similar to the value at solar neighborhood (Spitzer 1978). In this work, we assume that the dust-to-gas mass ratio is proportional to the metallicity (Draine et al. 2007). The dust mass m_{d} is given by $m_{\text{d}} = 4\pi a_d^3 \rho_{\text{d}}/3$, where ρ_{d} is the dust mass density. We assume $\rho_{\text{d}} = 3 \text{ g cm}^{-3}$ that is corresponding to a silicate dust grain. The dust size distribution in high-redshift galaxies has not been understood yet. In our Galaxy, the dust is likely to have a power-law size distribution $\frac{dn_{\text{d}}}{da_{\text{d}}} \propto a_{\text{d}}^{-3.5}$ with the size

range $\sim 0.01 - 1.0 \mu\text{m}$, so called the MRN size distribution (Mathis et al. 1977). In this work, we adopt a single dust size model with a fiducial value $a_d = 0.1 \mu\text{m}$. Note that, this single dust-size model is equivalent with the MRN dust model with the size range $8 \times 10^{-3} - 1.0 \mu\text{m}$ under the condition $Q_{d,\text{abs}} = 1$ (Yajima et al. 2017).

Thus, the traveling time $t_d = l_d/c$ is given by

$$t_d \sim 33 \text{ yr} \left(\frac{M_{\text{cl}}}{10^5 M_{\odot}} \right)^{-1} \left(\frac{r_{\text{cl}}}{5 \text{ pc}} \right)^3 \left(\frac{Z}{10^{-2} Z_{\odot}} \right)^{-1} \left(\frac{X_d}{0.1 \mu\text{m}^{-1}} \right)^{-1}, \quad (11)$$

here we define $X_d \equiv f_d/a_d$. When we consider the photon trapping time as t_d and substitute Eq. (11) into Eq. (3), the boost factor is evaluated as

$$f_{\text{boost,d}} = 2.0 \left(\frac{M_{\text{cl}}}{10^5 M_{\odot}} \right)^{-1} \left(\frac{r_{\text{cl}}}{5 \text{ pc}} \right)^2 \left(\frac{X_d}{0.1 \mu\text{m}^{-1}} \right)^{-1} \left(\frac{Z}{10^{-2} Z_{\odot}} \right)^{-1}. \quad (12) \text{Eq. (14):}$$

We estimate the trapping time of Ly α photons as $t_{\text{trap}} = \min(t_d, t_{\text{trap,H}})$. The critical metallicity that satisfies $t_{\text{trap,H}} = t_d$ is

$$Z_{\text{TP}} = 4.7 \times 10^{-5} Z_{\odot} \left(\frac{M_{\text{cl}}}{10^5 M_{\odot}} \right)^{-4/3} \left(\frac{r_{\text{cl}}}{5 \text{ pc}} \right)^{8/3} \left(\frac{X_d}{0.1 \mu\text{m}^{-1}} \right)^{-1}. \quad (13)$$

Note that, the momentum of Ly α photons is given to HI gas or dust at least once. Therefore, we take a higher value of the above estimation or unity as a minimum of f_{boost} . Fig. 1 shows the boost factor as a function of cloud radius. The dependence of cloud radius on the boost factor changes from $\propto r^2$ to $\propto r^{-2/3}$ at a specific radius that increases with metallicity as shown in Eq. (13). We find that the boost factor is regulated by the dust in the cases of compact clouds of which the mass and radius are similar to GCs. Therefore, we consider the boost factor as $f_{\text{boost}} = f_{\text{boost,d}}$ in cases with the metallicity higher than Z_{TP} .

Substituting Eq. (12) into Eq. (6), we finally obtain the critical value for the stellar-to-gas mass ratio (ξ_{crit}) above which the Ly α radiation feedback suppresses the star formation:

$$\xi_{\text{crit}} = 1.5 \left(\frac{\dot{n}_{\text{ion}}}{1 \times 10^{47} \text{ s}^{-1} M_{\odot}^{-1}} \right)^{-1} \left(\frac{M_{\text{cl}}}{10^5 M_{\odot}} \right)^2 \left(\frac{r_{\text{cl}}}{5 \text{ pc}} \right)^{-4} \times \left(\frac{X_d}{0.1 \mu\text{m}^{-1}} \right) \left(\frac{Z}{10^{-2} Z_{\odot}} \right). \quad (14)$$

The above estimation suggests that the star formation efficiency is regulated due to the Ly α radiative feedback as the metallicity decreases. Below, we investigate the critical condition for the metallicity.

If most of gas is evacuated due to the feedback, stars are likely to escape from the shallowed potential well. Hills (1980) analytically showed that star clusters became unbound if $\epsilon \lesssim 0.5$ (see also, Mathieu 1983). Then, Geyer & Burkert (2001) confirmed this critical condition by N -body simulations. Therefore, by considering the critical star formation efficiency as $\epsilon = 0.5$ (i.e., $\xi = 1$), we evaluate the critical metallicity Z_{crit} for forming bound star-clusters from

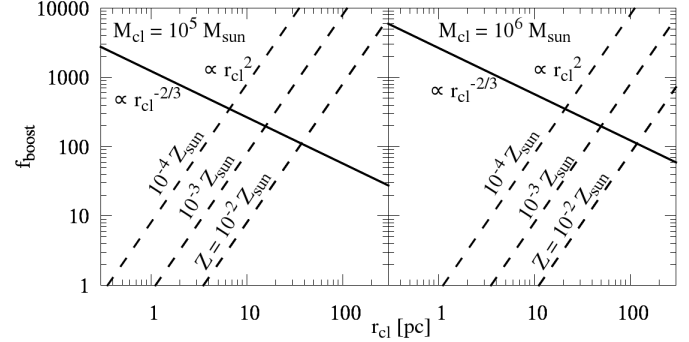


Figure 1. The boost factor as a function of cloud radius. Solid lines show the cases in which the dust absorption is not considered. Dash lines represent boost factors calculated by the trapping time until the optical depth of dust absorption becomes unity.

$$Z_{\text{crit}} = 6.6 \times 10^{-3} Z_{\odot} \left(\frac{\dot{n}_{\text{ion}}}{1 \times 10^{47} \text{ s}^{-1} M_{\odot}^{-1}} \right) \left(\frac{X_d}{0.1 \mu\text{m}^{-1}} \right)^{-1} \times \left(\frac{M_{\text{cl}}}{10^5 M_{\odot}} \right)^{-2} \left(\frac{r_{\text{cl}}}{5 \text{ pc}} \right)^4. \quad (15)$$

Note that there are uncertainties in modeling the parameter X_d . Nozawa et al. (2007) showed that the size distribution of dust in the early Universe tended to be biased toward the large size ($\gtrsim 0.1 \mu\text{m}$) since small grains were destroyed by the reverse shock of the supernova (SN) explosion. If we consider the dust size range as $0.1 \mu\text{m} < a_d < 1.0 \mu\text{m}$, the corresponding single dust size is $\sim 0.3 \mu\text{m}$. On the other hand, the typical dust size of the high- z galaxies has also been argued as smaller as $0.05 \mu\text{m}$ (Todini & Ferrara 2001; Dayal et al. 2010). Thus, X_d can be changed by a factor $\sim 0.5 - 3$.

In addition, the dust-to-gas mass ratio f_d can also change since the dust depletion factor in the early Universe (the mass ratio of dust to the total heavy elements) may be different compared to the local Universe. Schneider et al. (2012) estimated that the depletion factor as $\sim 3.4 \times 10^{-2}$ for the SN with the progenitor mass of $35 M_{\odot}$ and the metallicity of $Z/Z_{\odot} = 10^{-4}$, which was roughly corresponding to the tenth of the present-day depletion factor (Pollack et al. 1994; Schneider et al. 2012). Consequently, our dust parameter X_d can be ~ 3 times larger and/or ~ 10 times smaller than $X_d = 0.1 \mu\text{m}^{-1}$.

Fig. 2 shows the critical star formation efficiency as a function of metallicity. Shades represent the uncertainty of X_d as stated above, i.e., $0.01 < X_d < 0.3$. The dashed line parts represent $f_{\text{boost}} = 1$. In the case with the mass $10^5 M_{\odot}$ and the radius 5 pc , the SFE becomes smaller than ~ 0.5 for Salpeter IMF at the metallicity of $\log Z/Z_{\odot} \sim -2.5$, which nicely reproduces the lower bound of observed metallicity of GCs. Note that, for Larson IMF, the critical metallicity shifts higher side by a factor ~ 2 due to the higher production rate of Ly α photons. As the metallicity becomes lower than $\log Z/Z_{\odot} \sim -2.5$, Ly α photons are able to travel for a long time with multiple scatterings and exert the outward force on the gas, resulting in the small SFE. For the metallicity of $\log Z/Z_{\odot} = -4$ which is similar to observed

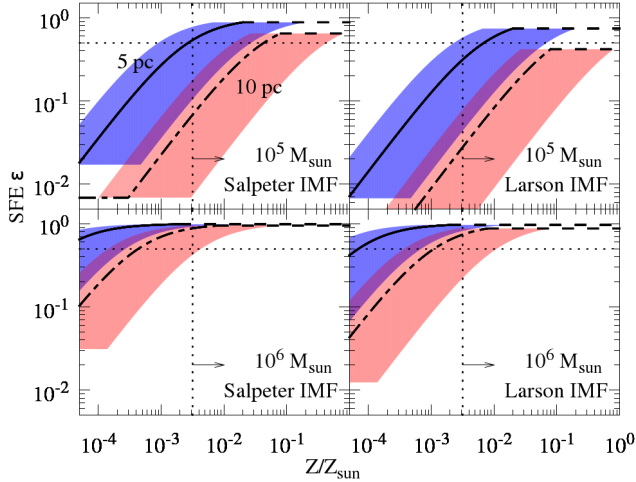


Figure 2. Critical star formation efficiency ϵ as a function of the metallicity Z , obtained by the Eq. (14). The star formation is suppressed by $\text{Ly}\alpha$ radiation feedback if the SFE exceeds the line. In each panel, solid and dashed-dotted lines correspond to the cloud radius of $r_{\text{cl}} = 5$ pc and 10 pc, respectively. As for each line, the fiducial dust model of $X_{\text{d}} = 0.1 \mu\text{m}^{-1}$ is adopted. The shaded regions represent the uncertainty of the dust model (see the text in detail). Dashed lines represent the minimum boost factor of $f_{\text{boost}} = 1$. Upper panels show the results for $M_{\text{cl}} = 10^5 M_{\odot}$ and lower panels are $M_{\text{cl}} = 10^6 M_{\odot}$. Left-hand and right-hand side panels show the results for the Salpeter and Larson IMF, respectively. Vertical dotted lines denote the lower bound of the observed metallicity of GCs, $\log Z/Z_{\odot} = -2.5$. The horizontal dotted lines represent $\epsilon = 0.5$. Note that the SFR becomes constant at $Z < Z_{\text{TP}}$ because of the constant traveling time of $\text{Ly}\alpha$ photons.

metal-poor stars, the SFE becomes $\epsilon \sim 3.6 \times 10^{-2}$ due to the large boost factor $f_{\text{boost}} \sim 200$. Therefore, stars formed in metal-poor gas are likely to disperse. Thus we suggest that GCs are difficult to form in metal-poor gas clouds. As the size of the cloud increases, i.e., the gas density decreases, the critical SFE becomes smaller because of the longer traveling time (see Eq. 11) and the shallower gravitational potential.

When the boost factor reaches unity, the critical SFE becomes constant to the metallicity as shown in Eq. (9). In the case with the cloud mass $10^6 M_{\odot}$, $\text{Ly}\alpha$ photons are absorbed by dust before they exert the strong radiation force on the gas, and the deeper gravitation potential can hold the gas against the feedback. As a result, the $\text{Ly}\alpha$ radiation feedback is insignificant even in the low-metallicity regions while the $\text{Ly}\alpha$ feedback begins to work (i.e., $f_{\text{boost}} > 1$) at the metallicity of $\log Z/Z_{\odot} \sim -2.5$. If we consider the radius of 10 pc and Larson IMF, the result seems to be reasonable to explain the observed lower bound of metallicity.

Next, we estimate the stellar density as $\rho_* \sim \frac{3M_*}{4\pi r_{\text{cl}}^3} = \frac{3\epsilon M_{\text{cl}}}{4\pi r_{\text{cl}}^3}$. By considering the metallicity dependence of the star formation efficiency (Eq. 14), we derive the stellar mass density as a function of metallicity as shown in Fig. 3. As the reference, we present the constant half-mass stellar density $\rho_{\text{h}} \equiv 3M_*/8\pi r_{\text{h}}^3$ for observed GCs (Portegies Zwart et al. 2010), assuming a mass-to-light ratio $M_*/L_{\text{V}} = 2$ (Pryor & Meylan 1993) and $[\text{Fe}/\text{H}] = Z/Z_{\odot}$. The observational data are taken from Harris (1996). Dotted lines represent the

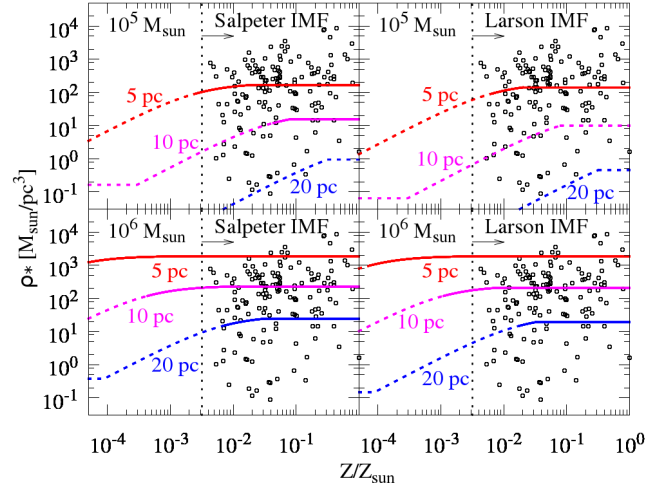


Figure 3. Stellar densities of star clusters as a function of the metallicity Z for each model of Fig. 2. Same as Fig. 2, vertical dotted lines denote the metallicity of $\log Z/Z_{\odot} = -2.5$. In each panel, solid, dashed-dotted and dashed-two dotted lines represent results for clouds with $r_{\text{cl}} = 5$ pc, 10 pc and 20 pc. Open circles indicate the constant half-mass density $\rho_{\text{h}} \equiv 3M_*/8\pi r_{\text{h}}^3$ (Portegies Zwart et al. 2010) for observed GCs (Harris 1996). In this figure, we assume the fiducial dust model of $X_{\text{d}} = 0.1 \mu\text{m}^{-1}$.

cases with $\epsilon < 0.5$. In these cases, stars become unbound after the gas evacuation. Therefore, only solid line parts should be considered in studying the stellar mass density. Note that, the estimated stellar density is the lower limit since the star clusters generally have the stellar density profile. For instance, if we assume the isothermal density profile ($\rho(r) \propto r^{-2}$ hence $M_*(r) \propto r$), the stellar density becomes four times larger if we estimate the stellar density at the half-mass radius. We see in the panels that the stellar densities decrease with the metallicity. This feature arises from the decreasing critical SFE, and the masses of formed star clusters become lower at given radii. We show some cloud models successfully reproduce the observed stellar density of GCs at the metallicity higher than $\log Z/Z_{\odot} \sim -2.5$, and the lower bound of the metallicity.

3 DISCUSSION AND CONCLUSIONS

In this Letter, we study the star formation in compact gas clouds under $\text{Ly}\alpha$ radiation feedback. We find that the $\text{Ly}\alpha$ radiation feedback significantly suppresses the star formation when the metallicity of the cloud is low. As the metallicity decreases, $\text{Ly}\alpha$ photons can be trapped in the cloud for a long time against dust absorption. In the journey of $\text{Ly}\alpha$ photons, they can exert the strong radiation pressure on the gas via multiple scattering processes, resulting in the disruption of clouds. If the star formation efficiency is smaller than ~ 0.5 , stars become unbound after the gas evacuation due to the radiation pressure or supernovae. Therefore, star formation is suppressed in metal-poor gas clouds, and compactly bound star clusters are unlikely to form. In the case of a cloud with the mass $10^5 M_{\odot}$ and the radius 5 pc, we show the critical metallicity for forming a bound star cluster is $\log Z/Z_{\odot} \sim -2.5$ above which more than half of gas can convert into stars. This critical metallicity is similar to the

lower bound of the observed metallicity of globular clusters (GCs). Thus we suggest that the Ly α radiation feedback can be a key roll in the formation of GCs.

In this work, we assume the simple dust model with the typical size of 0.1 μm and the constant dust-to-metal mass ratio normalized by that of the solar neighborhood. However, in the early Universe, the dust properties can significantly differ from local galaxies. This dust properties can also affect the formation of cloud properties due to the different thermal evolution of low-metal gas (e.g., Omukai et al. 2005). We will investigate the formation of dusty gas clumps by using cosmological hydrodynamics simulations with the evolution of dust properties in future work.

Our models are based on spherical gas clouds that are likely to trap Ly α photons efficiently. If Lyman continuum radiation from a star cluster makes ionized holes along low-density regions, Ly α photons can leak and the radiation force becomes weak. In addition, supersonic motion of gas, which is by turbulence or outflow, make the trapping time of Ly α photons shorter. These should be studied by multi-dimensional radiative-hydrodynamics simulations with Lyman continuum and Ly α line transfer calculations.

ACKNOWLEDGMENTS

We are grateful to H. Fukushima for fruitful discussion about the ionizing photon emissivity. We also thank the anonymous referee for useful comments that have improved the manuscript. This work is supported by MEXT/JSPS KAKENHI Grant Number 17H04827 (H.Y.).

REFERENCES

- Abe M., Umemura M., Hasegawa K., 2016, *MNRAS*, 463, 2849
- Adams T. F., 1975, *ApJ*, 201, 350
- Aoki W., Beers T. C., Christlieb N., Norris J. E., Ryan S. G., Tsangarides S., 2007, *ApJ*, 655, 492
- Bouwens R. J., van Dokkum P. G., Illingworth G. D., Oesch P. A., Maseda M., Ribeiro B., Stefanon M., Lam D., 2017, *ArXiv e-prints*
- Chen Y., Bressan A., Girardi L., Marigo P., Kong X., Lanza A., 2015, *MNRAS*, 452, 1068
- Cox D. P., 1985, *ApJ*, 288, 465
- Dayal P., Hirashita H., Ferrara A., 2010, *MNRAS*, 403, 620
- Diemand J., Madau P., Moore B., 2005, *MNRAS*, 364, 367
- Dijkstra M., Loeb A., 2008, *MNRAS*, 391, 457
- Dotter A., Chaboyer B., Jevremović D., Baron E., Ferguson J. W., Sarajedini A., Anderson J., 2007, *AJ*, 134, 376
- Draine B. T., Dale D. A., Bendo G., Gordon K. D., Smith J. D. T., Armus L., Engelbracht C. W., Helou G., Kennicutt Jr. R. C., Li A., Roussel H., Walter F., Calzetti D., Moustakas J., Murphy E. J., Rieke G. H., Bot C., Hollenbach D. J., Sheth K., Teplitz H. I., 2007, *ApJ*, 663, 866
- Draine B. T., Lee H. M., 1984, *ApJ*, 285, 89
- Geen S., Soler J. D., Hennebelle P., 2017, *MNRAS*, 471, 4844
- Geyer M. P., Burkert A., 2001, *MNRAS*, 323, 988
- Harris W. E., 1996, *AJ*, 112, 1487
- Hasegawa K., Umemura M., Kitayama T., 2009, *MNRAS*, 397, 1338
- Hills J. G., 1980, *ApJ*, 235, 986
- Kim J.-h., Ma X., Grudić M. Y., Hopkins P. F., Hayward C. C., Wetzel A., Faucher-Giguère C.-A., Kereš D., Garrison-Kimmel S., Murray N., 2017, *ArXiv e-prints*
- Krauss L. M., Chaboyer B., 2003, *Science*, 299, 65
- Kravtsov A. V., Gnedin O. Y., 2005, *ApJ*, 623, 650
- Mathieu R. D., 1983, *ApJ*, 267, L97
- Mathis J. S., Rimpl W., Nordsieck K. H., 1977, *ApJ*, 217, 425
- Moore B., Diemand J., Madau P., Zemp M., Stadel J., 2006, *MNRAS*, 368, 563
- Nozawa T., Kozasa T., Habe A., Dwek E., Umeda H., Tomiyaga N., Maeda K., Nomoto K., 2007, *ApJ*, 666, 955
- Oh S. P., Haiman Z., 2002, *ApJ*, 569, 558
- Omukai K., Tsuribe T., Schneider R., Ferrara A., 2005, *ApJ*, 626, 627
- Pollack J. B., Hollenbach D., Beckwith S., Simonelli D. P., Roush T., Fong W., 1994, *ApJ*, 421, 615
- Portegies Zwart S. F., McMillan S. L. W., Gieles M., 2010, *ARA&A*, 48, 431
- Pryor C., Meylan G., 1993, in *Astronomical Society of the Pacific Conference Series*, Vol. 50, *Structure and Dynamics of Globular Clusters*, Djorgovski S. G., Meylan G., eds., p. 357
- Puzia T. H., Perrett K. M., Bridges T. J., 2005, *A&A*, 434, 909
- Rees M. J., Ostriker J. P., 1977, *MNRAS*, 179, 541
- Renzini A., 2017, *MNRAS*, 469, L63
- Ricotti M., Parry O. H., Gnedin N. Y., 2016, *ApJ*, 831, 204
- Schneider R., Omukai K., Bianchi S., Valiante R., 2012, *MNRAS*, 419, 1566
- Smith A., Bromm V., Loeb A., 2017, *MNRAS*, 464, 2963
- Spitzer L., 1978, *Physical processes in the interstellar medium*
- Todini P., Ferrara A., 2001, *MNRAS*, 325, 726
- Trenti M., Vesperini E., Pasquato M., 2010, *ApJ*, 708, 1598
- VandenBerg D. A., Brogaard K., Leaman R., Casagrande L., 2013, *ApJ*, 775, 134
- Vanzella E., Calura F., Meneghetti M., Mercurio A., Castellano M., Caminha G. B., Balestra I., Rosati P., Tozzi P., De Barros S., Grazian A., D’Ercole A., Ciotti L., Caputi K., Grillo C., Merlin E., Pentericci L., Fontana A., Cristiani S., Coe D., 2017, *MNRAS*, 467, 4304
- Yajima H., Khochfar S., 2014, *MNRAS*, 441, 769
- , 2017, *MNRAS*, 467, L51
- Yajima H., Li Y., Zhu Q., Abel T., 2012, *MNRAS*, 424, 884
- Yajima H., Ricotti M., Park K., Sugimura K., 2017, *ApJ*, 846, 3
- Yong D., Norris J. E., Bessell M. S., Christlieb N., Asplund M., Beers T. C., Barklem P. S., Frebel A., Ryan S. G., 2013, *ApJ*, 762, 26